

## SUPPLEMENTARY INFORMATION

# Charge transfer in mixed and segregated stacks of tetrathiafulvalene, tetrathianaphthalene and naphthalene diimide: a structural, spectroscopic and computational study

Chanel F. Leong,<sup>a</sup> Bun Chan,<sup>b</sup> Tianfu Liu,<sup>c</sup> Harrison S. Moore,<sup>a</sup> Idan Hod,<sup>c</sup> Marcello B. Solomon,<sup>a</sup> Pavel M. Usov,<sup>a</sup> Joseph T. Hupp,<sup>c</sup> Omar Farha,<sup>c</sup> Deanna M. D'Alessandro<sup>a</sup>

## TABLE OF CONTENTS

<b>Optical Microscopy</b> .....	<b>S2</b>
<b>Crystallography</b> .....	<b>S3</b>
<b>Powder X-Ray Diffraction</b> .....	<b>S5</b>
<b>Electrochemistry</b> .....	<b>S6</b>
<b>UV-Vis-NIR Spectroscopy</b> .....	<b>S7</b>
<b>Raman Spectroscopy</b> .....	<b>S8</b>
<b>EPR Spectroscopy</b> .....	<b>S9</b>
<b>Conductivity</b> .....	<b>S10</b>

## Optical Microscopy and Crystallography

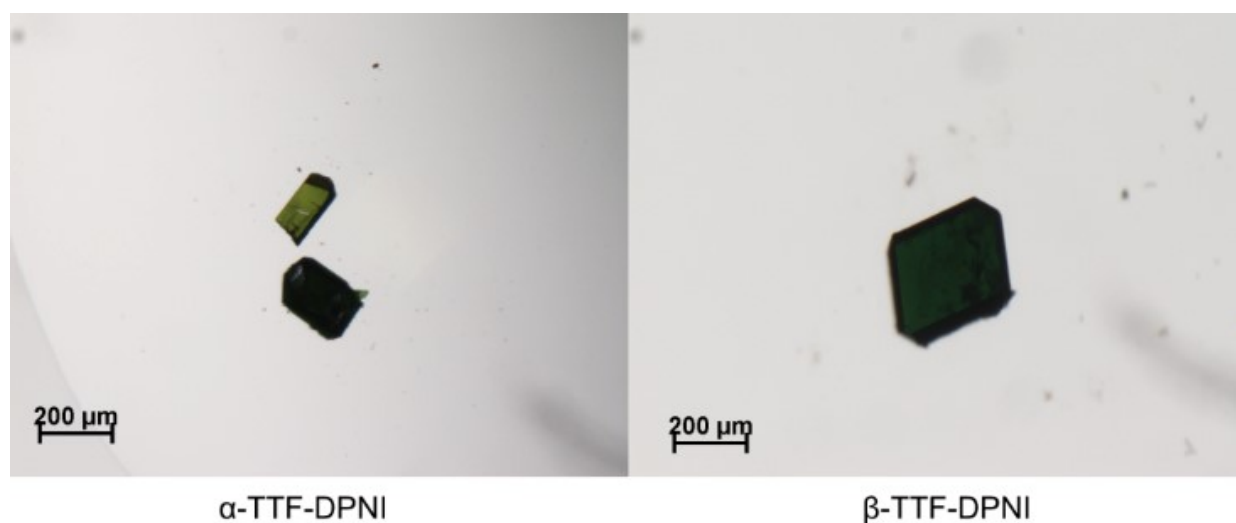


**Figure S1.** Microscope images of  $\alpha$ -TTF-DPNI (left) and  $\beta$ -TTF-DPNI (right). The dichroism of  $\alpha$ -TTF-DPNI due to polarisation of the light source is shown on the left.

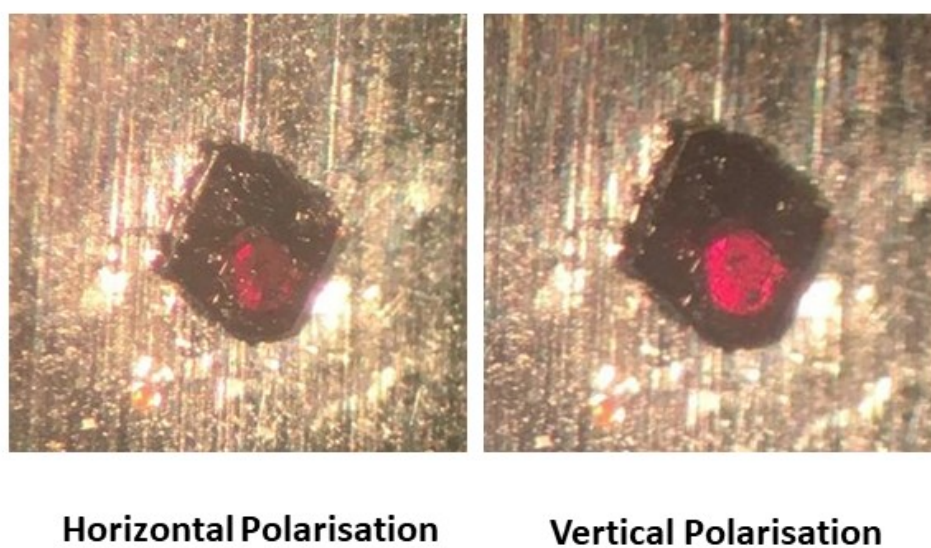


**Figure S2.** Microscope images  $\alpha$ -TTF-DPNI prior to (left) and following plane polarisation. While not as dramatic as the  $\alpha$ -TTF-DPNI CT complex, a lightening in crystal colour from black to red is still observable.

## Crystallography

**Table S1.** Crystallographic data for  $\alpha$ -TTF-DPNI,  $\beta$ -TTF-DPNI, and TTN-DPNI.

<i>Parameter</i>	<b><math>\alpha</math>-TTF-DPNI</b>	<b><math>\beta</math>-TTF-DPNI</b>	<b>TTN-DPNI</b>
<i>Empirical formula</i>	C <sub>60</sub> H <sub>32</sub> N <sub>8</sub> O <sub>8</sub> S <sub>8</sub>	C <sub>15</sub> H <sub>8</sub> N <sub>2</sub> O <sub>2</sub> S <sub>2</sub>	C <sub>15</sub> H <sub>8</sub> N <sub>2</sub> O <sub>2</sub> S <sub>2</sub>
<i>Formula weight</i>	1249.42	312.36	312.36
<i>Temperature (K)</i>	150	150	299
<i>Crystal system</i>	Triclinic	Monoclinic	Monoclinic
<i>Space group</i>	<i>P</i> -1	<i>P</i> 2 <sub>1</sub> / <i>c</i>	<i>P</i> 2 <sub>1</sub> / <i>c</i>
<i>a</i> (Å)	11.094	13.3254	14.044
<i>b</i> (Å)	11.346	8.47110	8.232
<i>c</i> (Å)	22.454	11.82420	11.711
<i>α</i> (°)	102.51	90	90
<i>β</i> (°)	97.53	101.0860	103.51
<i>γ</i> (°)	100.71	90	90
<i>Volume</i> (Å <sup>3</sup> )	2667.6	1309.82	1316.4
<i>Z</i>	2	2	2
<i>ρ<sub>calc</sub></i> (mg mm <sup>-3</sup> )	1.555	1.264	1.586
<i>μ</i> (mm <sup>-1</sup> )	3.673	3.602	3.722
<i>F</i> (000)	1280	508	648
<i>Crystal size</i> (mm)	0.03 × 0.01 × 0.01	0.10 × 0.08 × 0.06	0.06 × 0.03 × 0.02
<i>2θ range for data collection</i>	4.096 to 136.626°	6.76 to 151.79°	6.472 to 136.522°
<i>Reflections collected</i>	23781	24515	11251
<i>Data/restraints/parameters</i>	9250/0/757	2725/0/222	2375/0/190
<i>Goodness-of-fit on F<sup>2</sup></i>	0.882	0.855	1.052
<i>Final R indices [I ≥ 2σ(I)]</i>	R <sub>1</sub> = 0.0848	R <sub>1</sub> = 0.0282	R <sub>1</sub> = 0.0292
<i>Final R indices [all data]</i>	R <sub>1</sub> = 0.0880, wR <sub>2</sub> = 0.882	R <sub>1</sub> = 0.0295, wR <sub>2</sub> = 0.0756	R <sub>1</sub> = 0.0296, wR <sub>2</sub> = 1.052
<i>Largest diff. peak/hole/e</i> <i>Å<sup>-3</sup></i>	0.579/-0.764	0.325/-0.322	0.195/-0.221

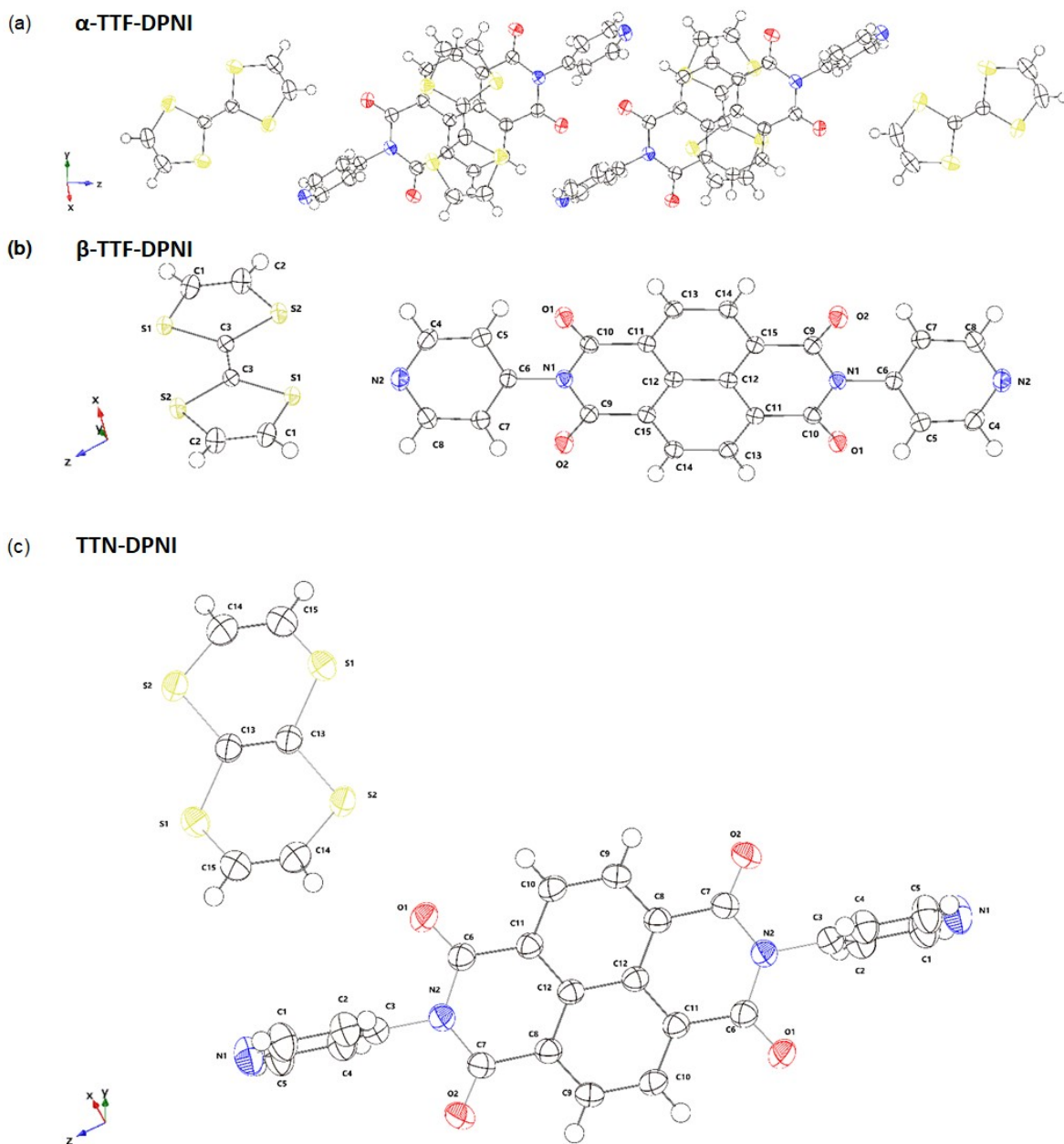


**Figure S3.** ORTEP depictions of (a)  $\alpha$ -TTF-DPNI, (b)  $\beta$ -TTF-DPNI and (c) TTN-DPNI. Note that atom labels have been left off  $\alpha$ -TTF-DPNI to improve clarity of the image. Colour scheme: N, blue; O, red; C, white; S, yellow; H, white circles.

## Powder X-Ray Diffraction

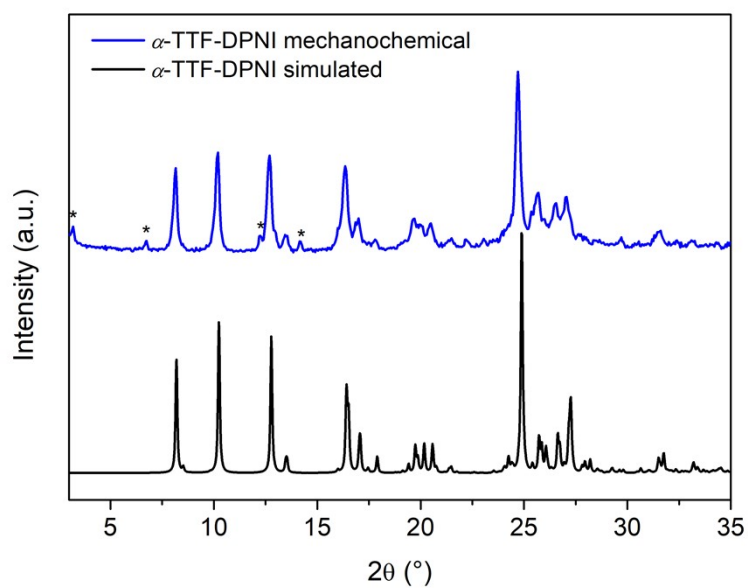


**Figure S4.** Simulated PXRD of  $\alpha$ -TTF-DPNI and PXRD of  $\alpha$ -TTF-DPNI prepared *via* mechanochemical synthesis. Asterisks indicate impurity/second phase.

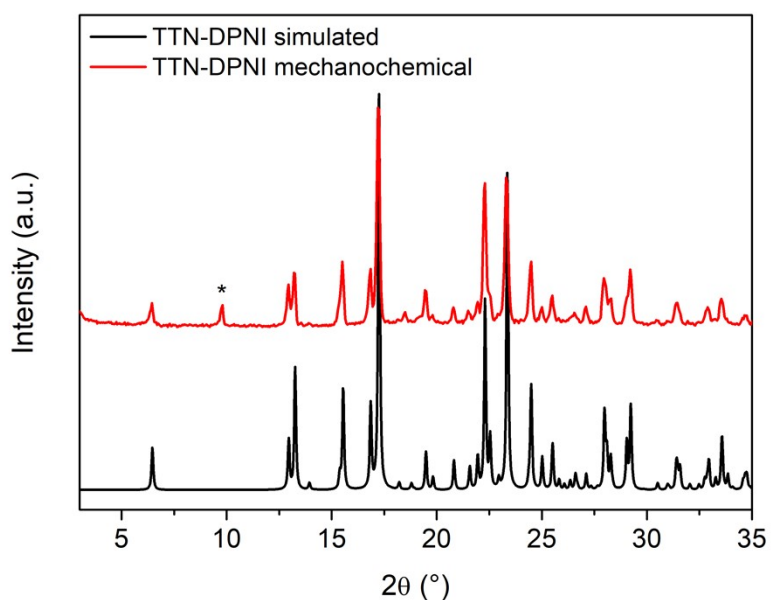


**Figure S5.** Simulated PXRD of TTN-DPNI and PXRD of TTN-DPNI prepared *via* mechanochemical synthesis. Asterisks indicate impurity.

## Electrochemistry

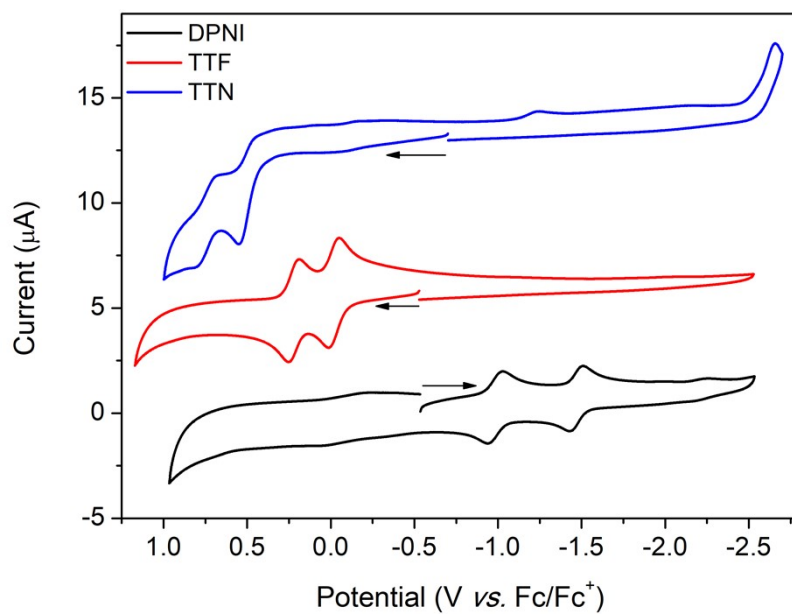


**Figure S6.** Solution state CV of DPNI, TTF and TTN collected at 100 mV/s in 0.1 M TBAPF<sub>6</sub>/DMF electrolyte. Potentials references to the Fc/Fc<sup>+</sup> redox couple. Arrows indicate the direction of forward scan.

## UV-Vis-NIR Spectroscopy

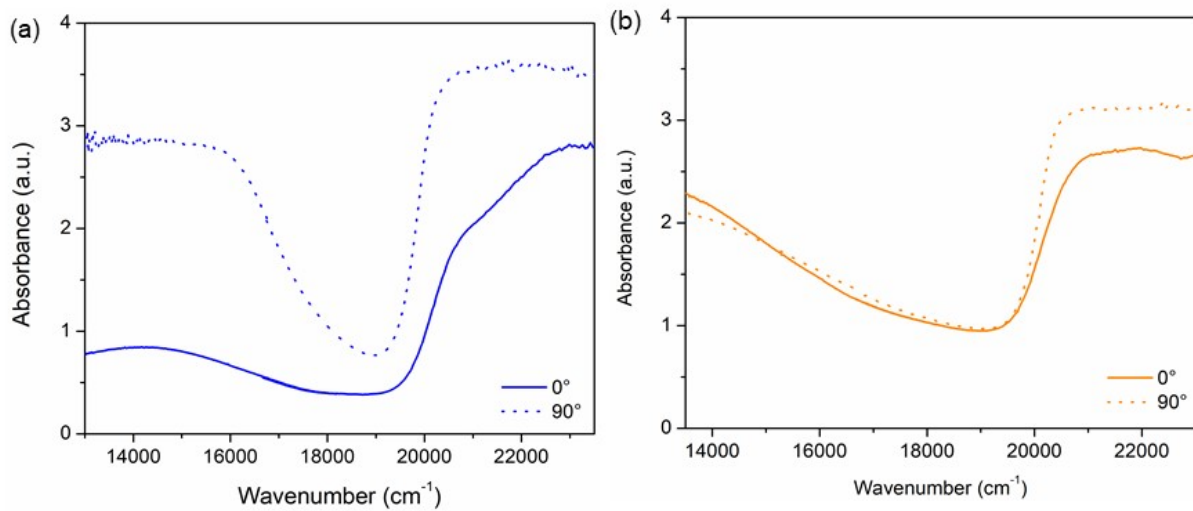


**Figure S7.** Single-crystal spectra of (a)  $\alpha$ -TTF-DPNI in the NIR region (b)  $\beta$ -TTF-DPNI in the visible region

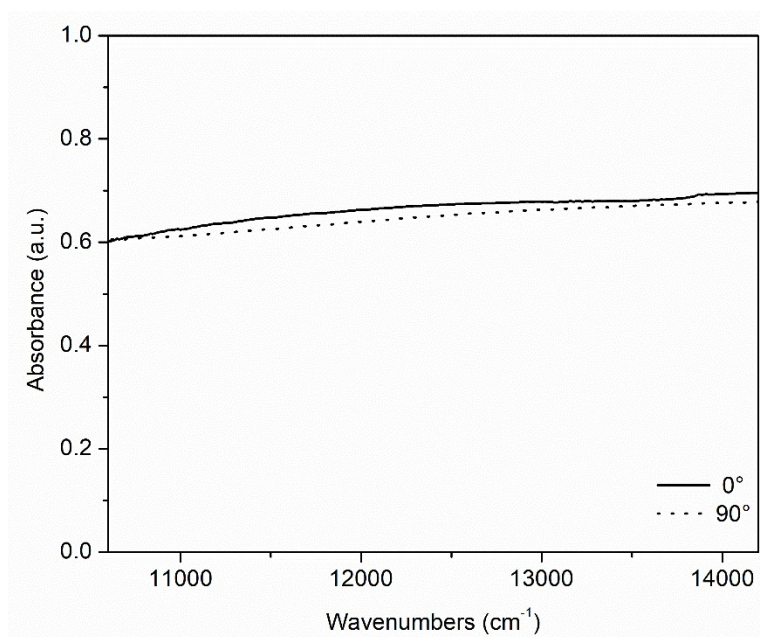


**Figure S8.** Single-crystal spectra of TTN-DPNI in the NIR region

## Raman Spectroscopy

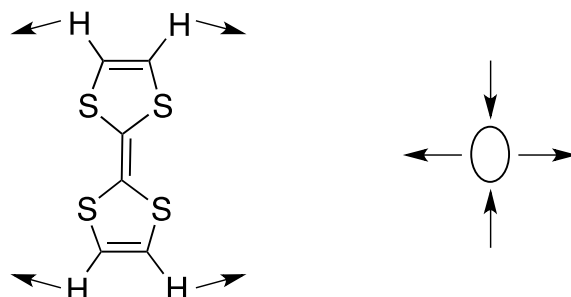


**Figure S9.** C-H bending mode in TTF that corresponds to its peak at  $\sim 1100 \text{ cm}^{-1}$  in the calculated Raman spectrum, and the change in shape of its polarisability ellipsoid.



## EPR Spectroscopy

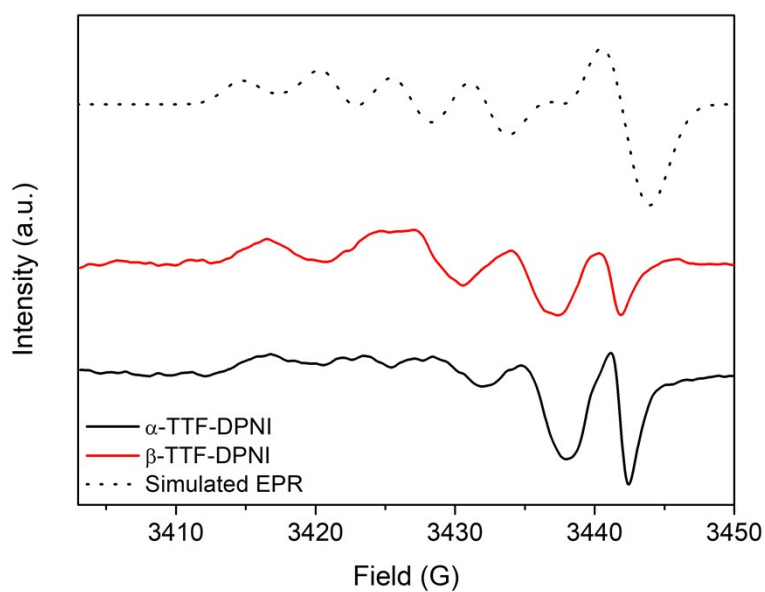


**Figure S10.** Experimental room temperature X-band EPR spectra of  $\alpha$ -TTF-DPNI and  $\beta$ -TTF-DPNI and a model EPR spectrum simulated using the EasySpin package on MATLAB.

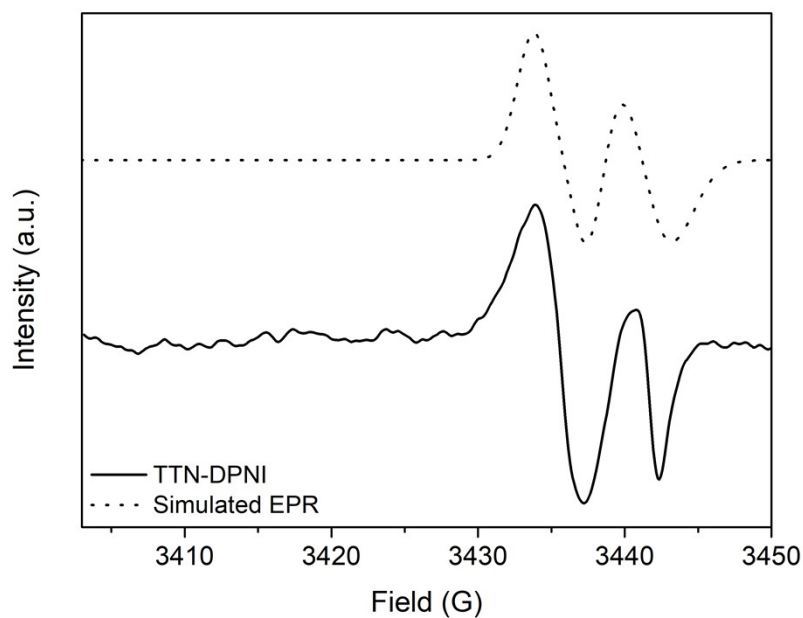


**Figure S11.** Experimental room temperature X-band EPR spectrum of TTN-DPNI and a model EPR spectrum simulated using the EasySpin package on MATLAB.

## Conductivity

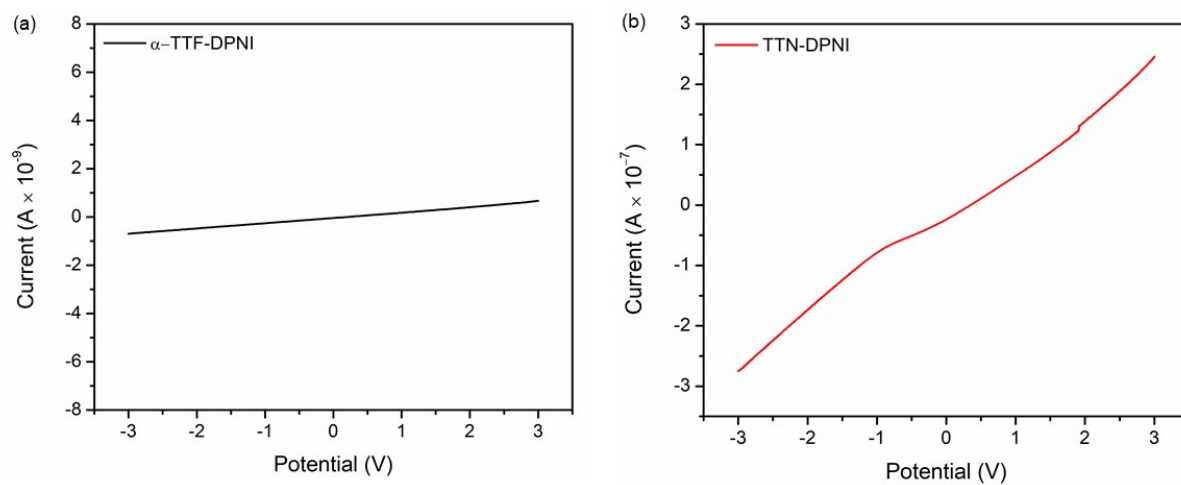


**Figure S12.** I–V curves of (a)  $\alpha$ -TTF-DPNI and (b) TTN-DPNI obtained *via* the two-probe method at room temperature.